ACOUSTICS 2012

Scholte-Stoneley waves on corrugated surfaces and on phononic crystal gratings

R. P. Moiseyenko[a], J. Liu[b], S. Benchabane[a], N. F. Declercq[b] and V. Laude[a]

[a]Femto-st, 32 avenue de l'Observatoire, 25044 Besancon, France
[b]Georgia Tech - CNRS, Metz Technopôle 2-3 rue Marconi 57070 Metz
rayisa.moiseyenko@femto-st.fr

Scholte-Stoneley waves (SSW) propagate at the interface of a fluid medium and a solid medium. They have a velocity smaller than the transverse and longitudinal velocities in the solid, and smaller than the sound velocity in the fluid. They are thus doubly evanescent and propagate without loss along the interface. They were observed for periodically corrugated surfaces in contact with water, with the periodic corrugation allowing their conversion from an incident plane wave generated by an ultrasound transducer. We consider in this work 1D silicon-water phononic crystals (PC) and study bulk wave to SSW modal conversion at the PC surface. PC are artificial periodic structures composed of at least two different materials. They are generally considered because of the existence of band gaps, i.e., frequency ranges for which wave propagation through the PC is prohibited. As diffraction gratings, they can also be used for the generation of SSW, as we show by looking for the incidence and frequency conditions for which they are excited.

1 Introduction

Conversion of longitudinal waves in fluids to surface waves at the interface with a solid has received much attention. Two surface waves, the generalized Rayleigh wave and the Scholte-Stoneley wave (SSW), may propagate at a plane solid-liquid interface [3]. Results are well established when the fluid sound velocity c_F is lower than the velocities of both bulk shear waves c_S and bulk longitudinal waves c_L in the solid. In that case, the generalized Rayleigh wave propagates with a phase velocity slightly lower than c_S and radiates energy into the fluid. In contrast, the Scholte-Stoneley wave propagates along the boundary with a phase velocity less than bulk velocities in water and in the solid. Therefore its energy and particle displacement are localized mostly in fluid, and slightly in the solid. Nevertheless, SSW theoretically predicted for smooth surface cannot be excited in experiments by plane sound waves incident from water. For this reason, recent studies on SSW have instead focused on corrugated surfaces. SSW have been studied in the 1980's for acoustic communication in shallow water and for non destructive testing (NDT) of materials because Scholte-Stoneley waves have a real velocity and as a consequence do not leak energy and propagate therefore over very large distances, while sticking to the surface. Based on experimental observations with a corrugated brass plate, SSW was suggested as a possible cause for the backward beam displacement effect. In this picture, the frequency at which the effect occurs is that of the diffraction of a Scholte-Stoneley wave backward propagating along the surface of the grating. [5, 2, 1]

In this paper, we consider the conditions for which SS waves appear on a corrugated fluid-solid interface, in the case of a silicon-water surface. The paper is organized as follows. First, calculations are made of the reference SSW velocity for the case of a smooth (non corrugated) fluid-solid interface. Next, a prediction of the angles for generation of SSW for a fixed frequency is made using numerical computations based on the finite element method. These predictions are compared with experimental results, obtained in the form of diffraction angular spectrograms for several angles of incidence. We end with some conclusions.

2 Theoretical study

2.1 Scholte-Stoneley velocity without corrugation

A detailed survey of the roots corresponding to the Rayleigh and Scholte-Stoneley surface waves of the Scholte-Stoneley equation was presented by Padilla [4]. We used his method

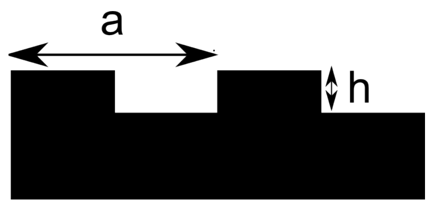

Figure 1: Corrugation profile.

Table 1: Bulk velocities and SSW velocity for silicon and water.

Material	ρ (kg/m^3)	c_L (m/s)	c_S (m/s)	c_{ss} (m/s)
Water	1000	1480	–	
Silicon	2329	8400	6000	1479.4

for the theoretical estimation of the Scholte-Stoneley velocity c_{ss}. for the case of a plane silicon surface immersed in water. If the sound velocities satisfy $c_{ss} < c_F < c_S < c_L$, the Scholte-Stoneley equation is solved as

$$S(k_x) = k_{Fz}[4k_x^2 k_{Sz} k_{Lz} + (k_S^2 - 2k_x^2)^2] - \rho k_S^4 k_{Lz} = 0 \quad (1)$$

where

$$\rho = \rho_{Fluid}/\rho_{Solid}$$

$$k_{iz} = \sqrt{k_i^2 - k_x^2}, \quad i = F, L, S$$

where F refers to the fluid, S to shear waves in the solid, L to longitudinal waves in the solid, and

$$k_i = \omega/c_i.$$

The SSW phase velocity is

$$c_{ss} = \omega/k_x.$$

It should be remarked that the obtained SSW velocity for a smooth surface differs from the case of a corrugated surface, but it gives at least a first approximation for prediction of incident angles for SSW generation.

2.2 Incidence angle for SSW generation

The optimum angle of incidence for the generation of a diffracted backward propagating lateral wave (i.e. a surface wave with velocity v_{ss} from Tab. 1) is given by Breazeale [5] as

$$\sin\theta_i = c_F\left(\frac{n}{fa} - \frac{1}{v_{ss}}\right) \quad (2)$$

with n the diffraction order. If we fix the angle at 40 deg. (50 deg.), two pairs of frequencies, 9 and 18 MHz (8.4 and 16.8 MHz) are found for orders of diffraction 1 and 2. Each pair corresponds to SSW generation in the first and the second order of diffraction of the surface grating.

2.3 FEM simulation for the corrugated surface

The experiments of the next section are numerically modeled by the finite element method at a given frequency, as shown in Figures 2 and 3. A fluid-structure interaction model is implemented. The circular domain encloses the water region surrounding the immersed silicon corrugated plate with parameters $a = 100\,\mu$m and $h = 200\,\mu$m. The plate thickness is 500 μm. Since we consider a finite fluid domain, radiation boundary conditions are imposed on the outer circle in order to prevent backward reflections. The transducer is modeled as a rectangle with three fixed sides and a fourth moving boundary. For the fourth side, we consider emission of compressional waves by imposing the boundary acceleration. Finite element simulations are performed for the selected frequencies at angles calculated in the previous subsection. Results are presented in Figs. 2 and 3 showing the pressure distribution at the considered frequency and angle of incidence. Incident, zero-diffraction order waves and backward propagating surface waves are clearly visible in Fig. 2a ($f = 9$ MHz, $\theta_i = 40^o$). In Fig. 3a, however, the backward propagating surface waves seem absent ($f = 8.4$ MHz, $\theta_i = 50^o$), suggesting the Padilla SSW velocity might not be close to the corrugated SSW velocity in this case. In Figs. 2b and 3b, the second order backward propagating surface waves are clearly visible, where the operating conditions were selected using Breazeale's formula and the Padilla SSW velocity.

3 Experimental diffraction results

The sample was fabricated on a silicon wafer of 500 micron thickness in the technology center of Femto-ST. The corrugation is defined by a mask that is transferred to a resist layer by deep UV lithography. After removal of the exposed resist, silicon is deep-etched in a reactive ion etching machine. The corrugation width is $a = 100\,\mu$m and the height is $h = 200\,\mu$m (Fig. 1). The aspect ratio is better than 20, meaning that the walls of the corrugation are vertical to within 1^o.

Diffraction measurements were done using a Polar C-scan apparatus at Georgia Tech Lorraine. The sample was immersed in a tank filled with water. A pair of transducers of nominal central frequency 15 MHz and wide bandwidth was used for the measurements. Their transmission spectrum in the absence of a sample is presented in Fig. 4. The emission beam width is about 10 mm. The emitting transducer is kept fixed and the receiving transducer is mounted on a rotating fork attached to the Polar/C-scan robot. The angular range of the fork rotation is from -55 to 55 degrees. During the experiments, this range was limited from -40 to 40 degrees. Diffraction measurements consist of the collection of time-waveforms at the different diffraction angles. The angular resolution for scans obtained using pulsed ultrasound is 0.1 degree under our experimental conditions.

Prior to this work, a numerical study of the behavior of Scholte-Stoneley waves when they encounter the corner of a solid plate revealed that hey are scattered in the forward direction upon reaching the corner [8]. Hence, they do not propagate around the corner, as would be expected from leaky Rayleigh waves. This phenomenon has been observed experimentally [7]. This radiation property allows us to measure the occurrence of Scholte-Stoneley waves by observation of the sound field at 90 degrees from incidence.

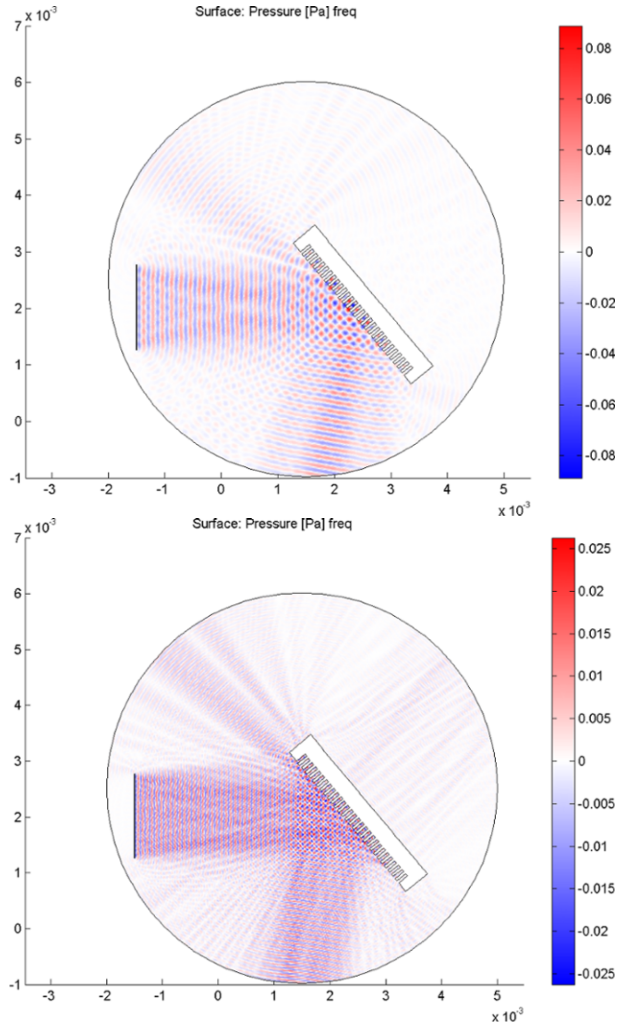

Figure 2: Finite element simulation of diffraction of a plane pressure wave incident on a corrugated silicon plate. Pressure distributions are shown at incidence angle $\theta_i = 40^o$, and frequencies 9 MHz (top) and 18 MHz (bottom). The corrugated silicon plate has parameters a=100 μm and h=200 μm.

Experimental results as angular scans are presented in Fig. 6. Dotted lines represent the dispersion of diffraction orders, as obtained from the grating law in water:

$$\sin\theta_m + \sin\theta_i = m\frac{c_F}{fa} \tag{3}$$

with c_F the velocity of acoustic waves in the surrounding fluid medium, f the frequency, and m the index of the considered diffraction order. It has to be stressed that the fluid velocity appears in this formula for the diffracted order, instead of the SSW velocity in Breazeale's equation (2).

The possibility of surface wave generation at normal incidence was considered earlier theoretically in the general inhomogeneous wave case for the brass-water interface [6]. At every frequency corresponding to an intersection of these lines with the dispersion curves, an anomaly was observed. It was found that Scholte-Stoneley wave generation is related to cut-off frequencies for the diffraction order appearance. Our experimental angular spectrograms for oblique incidence confirm this conclusion. SS waves are found for the first and second diffraction orders.

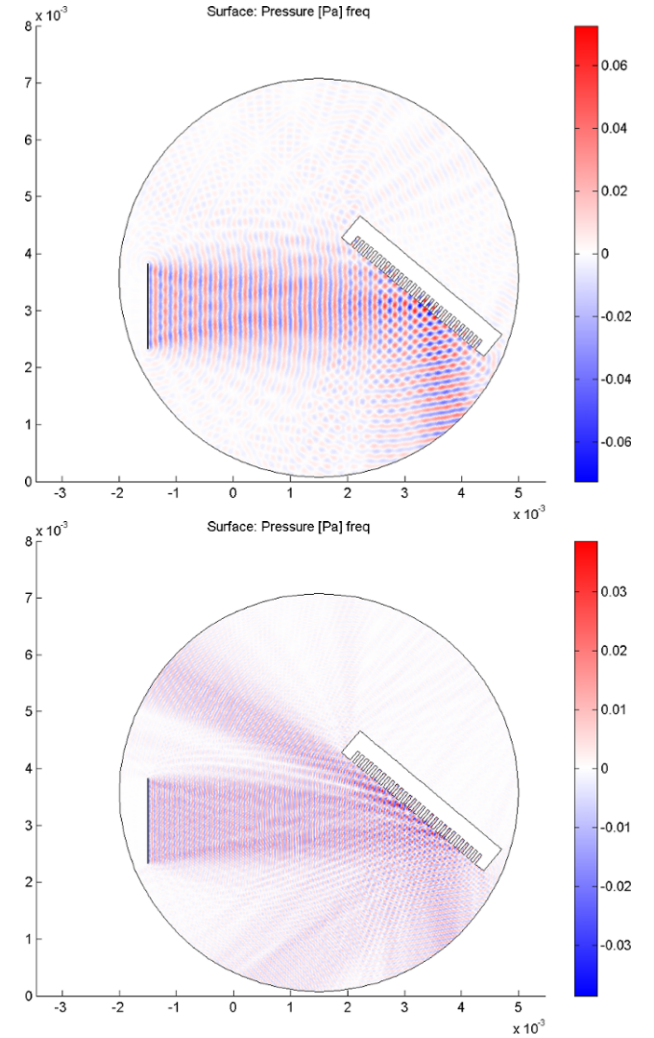

Figure 3: Finite element simulation of diffraction of a plane pressure wave incident on a corrugated silicon plate. Pressure distributions are shown at incidence angle $\theta_i = 50^o$, and frequencies 8.4 MHz (top) and 16.8 MHz (bottom). The corrugated silicon plate has parameters a=100 μm and h=200 μm.

.

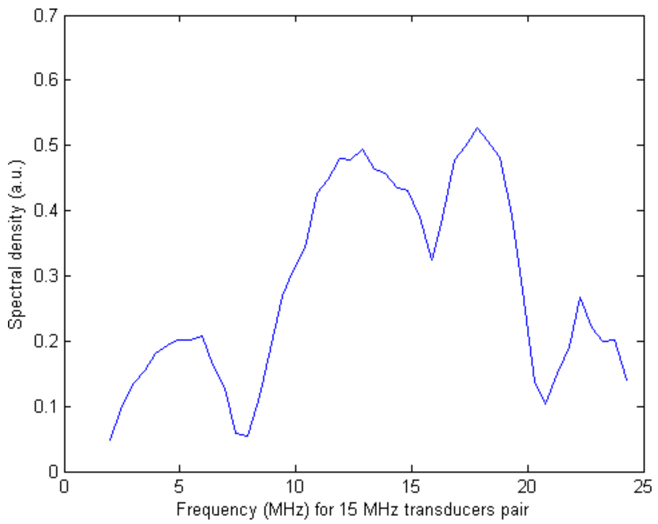

Figure 4: Experimental transmission as a function of frequency (in arbitrary units) for a transducer pair of 15 MHz central frequency.

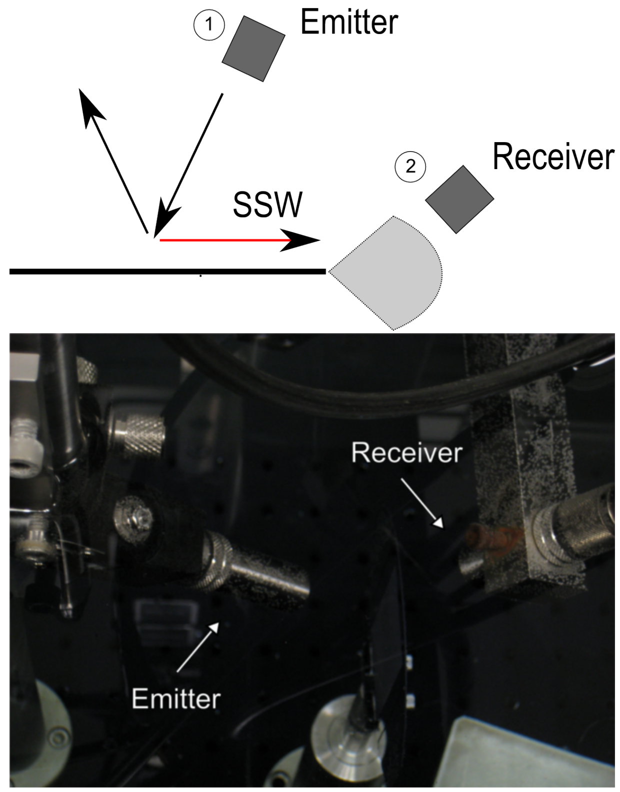

Figure 5: (top)Schematic drawing for diffraction measurements of Scholte-Stoneley waves. (bottom) Photograph of experimental setup showing the sample inside the tank filled with water and the mounts holding the transducers.

4 Conclusion

We have presented new experiments on corrugated surfaces. A theoretical and experimental investigation of the conditions for Scholte-Stoneley wave generation on a 1D corrugated silicon plate has been conducted. SS waves were generated through diffraction and were shown to be efficiently excited when the Breazeale phase matching condition is fulfilled. The obtained experimental results for oblique incidence extend the phenomena predicted for SSW generation in the case of normal incidence by other authors. We noticed the appearance of SS waves at cut-off frequencies slightly lower than diffraction order cut-off frequencies in water. Further investigations are under way to understand better the observed phenomena and their relationship with other guided wave phenomena on other samples. The obtained results could be applied to the design of novel transducers based on the conversion of compressional waves into surface waves. Another perspective is the further study of corrugated plates with extension to 2D corrugated grating structures.

Acknowledgments

Financial support by the Agence Nationale de la Recherche under grant ANR-09-BLANC-0167-01 is gratefully acknowledged.

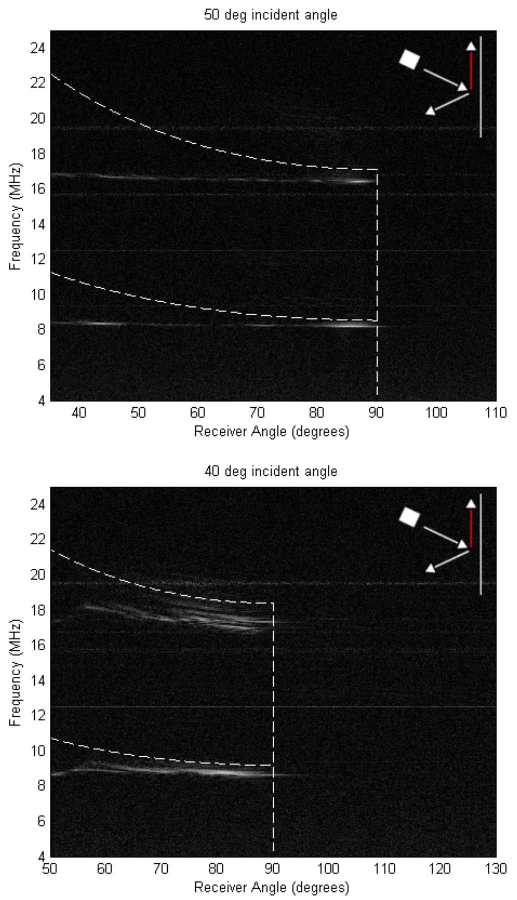

Figure 6: Angular spectrograms of diffracted waves. The incident angle $\theta_i = 40^o$ (top) and $\theta_i = 50^o$ (bottom), for the corrugated silicon plate immersed in water with $a = 100\ \mu$m and $h = 200\ \mu$m. First and second diffraction orders in water are represented by dotted lines.

References

[1] A. Teklu, M. A. Breazeale ,N. F. Declercq, R. D. Hasse, M. S. McPherson, "Backward displacement of ultrasonic waves reflected from a periodically corrugated interface", *J. Appl. Phys.* **97**, 084904 (2005)

[2] S. W. Herbison, J. M. Vander Weide, N. F. Declercq, "Observation of ultrasonic backward beam displacement in transmission through a solid having superimposed periodicity", *Applied Physics Letters* **97**, 041908 (2010)

[3] L. M.Brekhovskikh, *Waves in Layered Media*, Academic, New York, (1980).

[4] F. Padilla, M. de Billy, G. Quentin, "Theoretical and experimental studies of surface waves on solid–fluid interfaces when the value of the fluid sound velocity is located between the shear and the longitudinal ones in the solid", *J. Acoust. Soc. Am.* **106**, 666 (1999).

[5] M. A. Breazeale, M. A. Torbett, "Backward displacement of waves reflected from an interface having superimposed periodicity", *Appl. Phys. Lett.* **29**, 456 (1976).

[6] E.-A. V. D. Abeele, R. Briers, O. Leroy, "Inhomogeneous plane-wave scattering and mode stimulation on periodic rough surfaces", *J. Acoust. Soc. Am.* **99**, 2883 (1996).

[7] A. Tinel, J. Duclos, "Diffraction and conversion of the Scholte–Stoneley wave at the extremity of a solid", *J. Acoust. Soc. Am.* **95**, 13–20 Í(1994).

[8] R. Briers, O. Leroy, G. N. Shkerdin, "Conversion of a Stoneley wave at the extremity of a fluid loaded plate", *J. Acoust. Soc. Am.* **101**, 1347–1357 (1997).